JOURNAL OF SOLID STATE CHEMISTRY 2, 347–365 (1970)

Rare-Earth Ions in a Hexaognal Field I*

E. SEGAL AND W. E. WALLACE

Department of Chemistry, University of Pittsburgh, Pittsburgh, Pennsylvania 15213

Received December 19, 1969; Revised April 17, 1970

Energy levels, eigenfunctions, and magnetic moments of rare-earth ions in a crystal field of hexagonal symmetry have been obtained using a Hamiltonian of the form $\mathscr{H} = B_4^0 O_4^0 + B_6^0(O_6^0 + \frac{7}{8}O_6^6)$. Results have been presented for all J values appearing in the rare-earth series and have been tabulated in a form convenient for use in analyzing the influence of the crystal field on the bulk thermal and magnetic properties of compounds containing the rare earths. Since experiment shows that B_6^0/B_6^6 may deviate from 8/77, a few calculations were made with this ratio deviating by 10 and 20% (from 8/77). These calculations showed the results to be relatively insensitive to changes in B_6^0/B_6^6.

I. Introduction

For many years it has been apparent (*1–7*) that the macroscopic thermal and magnetic properties of systems containing rare earths are significantly influenced by the interaction between the rare-earth ion and the ions in its environment. Information has become available (*8*)[1] for assessing these effects for crystals having cubic symmetry but not for hexagonal crystals. The objectives in this study and in this manuscript are (1) to provide for hexagonal crystals information needed to assess the influence of the crystal field interaction on their heat capacity and susceptibility behavior, and (2) to present the results of the calculation in a form convenient for use by experimentalists. For simplicity the treatment is limited to hexagonal crystals having an ideal axial ratio.

When a free rare-earth ion is placed in a crystal, its $2J+1$ fold degeneracy is partially lifted through electrostatic interaction between its f-electrons and the charges on the surrounding ions. The multiplet is split into a number of states, which can appropriately be termed the crystal field (CF) states. The assemblage of rare-earth ions in the crystal is, of course, distributed over the CF states, the distribution at a given temperature and the temperature variation of the population of a given state both being governed by the Boltzmann expression. The variations in population of the various CF states which occur as a result of a change in temperature significantly affects a number of macroscopic properties of rare earth systems—their conductivities, thermal properties, and bulk magnetic characteristics. For example, if, as temperature is reduced, ions settle into states of low or vanishing moment, electrical conductivity substantially improves due to the suppression of spin-disorder scattering effects.

The influence of the crystal field on the temperature dependence of susceptibility (χ) was discussed by Penney and Schlapp (*2*) many years ago. χ may be computed from the fundamental Van Vleck equation

$$\chi = (N_0/H) \sum_i \mu_i \exp(-E_i/kT) / \sum_i \exp(-E_i/kT), \quad (1)$$

where N_0 = the Avogadro number, H represents field strength, and μ_i and E_i refer to the magnetic moment and energy, respectively, of the i-th crystal field level. Penney and Schlapp pointed out that for temperatures such that $kT > E_i$, Eq. (1) leads to a reciprocal susceptibility which is linearly dependent on T (Curie–Weiss behavior), whereas at lower temperatures such that this condition is no longer fulfilled significant deviations from linear behavior can occur. The effect of shifting populations in the various CF states is evident not only in the χ vs T

* This work was assisted by the U.S. Atomic Energy Commission and the Army Research Office, Durham, North Carolina.

[1] Our parameters x and W are not identical to that of this reference. Here the B_n^m or x and W are expressed in a coordinate system in which the z axis is along the cubic [100] direction. In the present paper z is along the hexagonal c axis corresponding to the cubic [111] direction.

behavior of rare-earth systems but also in their heat capacities. At very low temperatures ions occupy the lowest CF state(s). With increasing temperature excitation within the CF spectrum occurs, producing a significant contribution to the total heat capacity. This contribution (C_C) is given by the expression

$$C_C = RT^2 d^2 \ln Q/dT^2 \qquad (2)$$
$$\text{where } Q = \sum_i \exp(-E_k/kT).$$

Numerous studies of the susceptibility and heat capacity behavior of metallic rare-earth systems have been made in the last decade (*1–5*). Many of these have clearly revealed the crystal field effects just alluded to, the qualitative features being evident from the most superficial scrutiny. However, to evaluate the results quantitatively it is necessary to know E_i and μ_i and also the eigenfunctions (ψ_i) for the crystal field states. These quantities can be determined by straightforward calculational methods which are described very briefly in the next section. Thus, in principle it is possible to make *ab initio* calculations of C_C and χ; in practice they can be computed with useful precision only in parametrical form (with 1, 2, or 3 disposable parameters involved) because the quantities $\langle r^n \rangle$ with $n = 2$, 4, and 6 enter into the calculations and these expectation values for the *f* electrons are not known with sufficient precision to warrant direct calculation of macroscopic properties. One must instead be satisfield to show (*6, 7, 9, 10*) that with reasonable values of the parameters a proper accounting can be made for the temperature dependence of C_C and/or χ. Any "comparison" between theory and experiment then reduces to a process of evaluating the disposable parameters, from which can be obtained such important information as the overall splitting (E_c) and other details of the CF spectrum, the relative importance of different order terms in the perturbing potential, etc.—information which is of very considerable significance.

As a result of work extending over the preceding three decades adequate information is available (*2, 8, 11, 12*), to permit the analysis alluded to in the previous paragraph to be made for crystals of cubic symmetry. There is no correspondingly comprehensive treatment for crystalline systems of hexagonal symmetry, although a number of special cases have been solved (*5, 6, 13–15*[1]). Most of the early work pertained to chlorides and the triethyl sulfates in which the second order interaction is important. More recent work from this laboratory has been concerned with metallic systems involving Pr—elemental Pr and $PrAl_3$. These analyses have represented steps toward providing the much needed general information for hexagonal systems. The present work is an extension to include all other *J* values, but, as will be noted below, is restricted to crystals whose axial ratios are ideal. The treatment will be extended later to include the effect of an applied magnetic field (II in the series) and the influence of deviation from the ideal axial ratio so that the second-order term becomes important (III in the series).

In Section II very brief descriptions are given of the Hamiltonian employed and the mode of calculation. Results are presented in Section III together with some comments about possible errors which arise out of the approximate nature of the Hamiltonian.

[1] This monograph gives very extensive references to the pertinent literature (pp. 352–385).

II. General Description of the Calculations

A. The Hamiltonian

The most general Hamiltonian for a hexagonal crystal field contains four independent parameters. Following the notation described by Hutchings (*16*) it can be written

$$\mathcal{H} = B_2^0 O_2^0 + B_4^0 O_4^0 + B_6^0 O_6^0 + B_6^6 O_6^6. \qquad (3)$$

To date very few calculations have been made using this complete and complex Hamiltonian. If consideration is limited to crystals with the ideal axial ratio (i.e., $c/a = 2\sqrt{2/3} = 1.63$), the second-order term vanishes. The Hamiltonian can be further simplified by making use of the result $B_6^0/B_6^6 = \frac{8}{77} = 0.1035$ obtained if the point charge model applies.

$$\mathcal{H} = B_4^0 O_4^0 + B_6^0 (O_6^0 + \tfrac{77}{8} O_6^6). \qquad (4)$$

Calculations were made using this simplified Hamiltonian. Clearly these calculations can be regarded as significant only if the simplified Hamiltonian can be justified. It is appropriate to examine this point in some detail.

First, consider the axial ratio limitation. Are there materials of interest with ideal or nearly ideal (viz., B_2 very small) axial ratios? The answer to this question is yes. Elemental Pr ($c/a = 1.61$) is an example; it was recently analyzed (*5, 10*) on the basis of $B_2 = 0$ and excellent agreement with experiment was achieved. Other hexagonal elements and intercompounds with axial ratios which are ideal or nearly so: Ce, 1.62; Nd, 1.612; $ErMn_2$, 1.63;

$TmMn_2$, 1.63; $DyOs_2$, 1.61; $ErOs_2$, 1.65, etc. There are thus sufficient crystals known to warrant undertaking calculations with c/a restricted to the ideal values.

Next, consider the use of the assumed ratio for B_6^0/B_6^6. Calculations (*17*) show that this ratio is relatively insensitive to the positions of the surrounding ions so that small deviations in c/a from 1.63 are insignificant. This ratio is also insensitive to the model used in the calculations. The point charge model values are not too different from the values computed from the more general ionic model (*17*) which takes into account in addition to the point charges higher induced moments of the surrounding ions. Experiment reveals that this ratio is also relatively insensitive to the particular rare-earth ion and/or the nature of the substance involved. For example, assuming $B_6^0/B_6^6 = 0.1035$ led (*6, 10*) to a proper analysis of the magnetic and thermal properties of Pr and $PrAl_3$. In addition analysis of results for nine rare-earth trichlorides, whose structures differ markedly from those of Pr and $PrAl_3$, leads (*18*) to a ratio 0.100 and which is moreover constant to 3% over the entire group of rare-earth halides. Thus there is experimental support for the assumed relationship between B_6^0 and B_6^6. Nevertheless the possibility exists that B_6^0/B_6^6 may deviate from 0.1035 by 10% or more. To ascertain the effect of such variations some of the calculations were repeated with the ratio differing from 0.1035 by 10 or 20%. The influence of this variation, which was minor, will be discussed more fully in the following section.

B. The Energies, Eigenfunctions, and Magnetic Moments

If the crystal field interaction (E_c) is weak compared to the spin-orbit coupling energy, eigenfunctions for the crystal field states Γ_i can be expressed as linear combinations of eigenfunctions for the free ion associated with various M values, $|M\rangle = |LSJM\rangle$:

$$|\Gamma_i\rangle = \sum_{M=-J}^{J} a_{iM}|M\rangle. \tag{5}$$

Given the Hamiltonian, the Operator Equivalent method developed by Stevens (*19*) can be employed in a straightforward way to establish the eigenvalues and eigenfunctions [i.e., to evaluate numerically the a_i's in Eq. (5)]. A thorough discussion of the Operator Equivalent method has been given by Hutchings (*16*). Further information regarding details of the technique involved in making the present calculations may be found elsewhere (*20*).

TABLE 1

NOMENCLATURE USED IN EIGENFUNCTION DESIGNATION

Terms Appearing in Eigenfunction (See Eq. 5 in Text)	Dominant Term $J = 2n$	Designation
$\|0\rangle$, $\|6\rangle$, $\|-6\rangle$	$\|0\rangle$	*o*
$\|\pm1\rangle$, $\|\pm5\rangle$, $\|\pm7\rangle$	$\|\pm1\rangle$	*a*
$\|\pm2\rangle$, $\|\pm4\rangle$, $\|\pm8\rangle$	$\|\pm2\rangle$	*b*
$\|+3\rangle$, $\|-3\rangle$	$\|\pm3\rangle$	*c*
$\|\pm2\rangle$, $\|\pm4\rangle$, $\|\pm8\rangle$	$\|\pm4\rangle$	*d*
$\|\pm1\rangle$, $\|\pm5\rangle$, $\|\pm7\rangle$	$\|\pm5\rangle$	*e*
$\|0\rangle$, $\|+6\rangle$, $\|-6\rangle$	$\|\pm6\rangle$	*f*
$\|\pm1\rangle$, $\|\pm5\rangle$, $\|\pm7\rangle$	$\|\pm7\rangle$	*g*
$\|\pm2\rangle$, $\|\pm4\rangle$, $\|\pm8\rangle$	$\|\pm8\rangle$	*h*
	$J = 2n + 1$	
$\|\pm1/2\rangle$, $\|\pm11/2\rangle$, $\|\pm13/2\rangle$	$\|\pm1/2\rangle$	*a*
$\|\pm3/2\rangle$, $\|\pm9/2\rangle$, $\|\pm15/2\rangle$	$\|\pm3/2\rangle$	*b*
$\|\pm5/2\rangle$, $\|\pm7/2\rangle$	$\|\pm5/2\rangle$	*c*
$\|\pm5/2\rangle$, $\|\pm7/2\rangle$	$\|\pm7/2\rangle$	*d*
$\|\pm3/2\rangle$, $\|\pm9/2\rangle$, $\|\pm15/2\rangle$	$\|\pm9/2\rangle$	*e*
$\|\pm1/2\rangle$, $\|\pm11/2\rangle$, $\|\pm13/2\rangle$	$\|\pm11/2\rangle$	*f*
$\|\pm1/2\rangle$, $\|\pm11/2\rangle$, $\|\pm13/2\rangle$	$\|\pm13/2\rangle$	*g*
$\|\pm3/2\rangle$, $\|\pm9/2\rangle$, $\|\pm15/2\rangle$	$\|\pm15/2\rangle$	*h*

To facilitate discussion and presentation of data the nomenclature presented in Table 1 is adopted.

C. Magnetic Moments of the Crystal Field States

To facilitate the calculation of magnetic properties, the magnetic moment has been computed for each of the crystal field states. Moments parallel and perpendicular to the hexagonal axis are denoted $\mu_\parallel$ and $\mu_\perp$, respectively. The magnetic moment μ is given by the fundamental expression

$$\mu = \langle \Gamma_i | (\mu)_{op} | \Gamma_i \rangle \tag{6}$$

where $\mu_{op} = gJ$. From (6) one obtains for $\mu_\parallel$ the expression

$$\mu_\parallel = \frac{1}{J} \sum_{M=J}^{J} M a_M^2 \tag{7}$$

$\mu_\perp$ vanishes unless J is nonintegral and Γ_i contains terms corresponding to $\Delta M = \pm 1$. Under these circumstances $\mu_\perp$ may exceed $\mu_\parallel$. In general

$$\mu_\perp = \frac{1}{J} \langle \Gamma_i | J_x | \Gamma_i \rangle \tag{8}$$

and the contributions to $\mu_\perp$ come from the cross terms in Γ_i corresponding to $\Delta M = \pm 1$. The matrix elements involved in Eq. (8) are given by the expressions

$$\langle M | J_x | M + 1 \rangle = 1/2\sqrt{(J - M)(J + M + 1)} \tag{9a}$$

and

$$\langle M|J_x|M-1\rangle = 1/2\sqrt{(J+M)(J-M+1)}. \quad (9b)$$

For the special case that $\Gamma_i = |\pm 1/2\rangle$

$$\mu_\perp = \frac{1}{2J}(J+1/2). \quad (10)$$

Also for the levels a, f, and g for $J = 15/2$, which involve the cross terms $M = \pm 11/2$ and $\pm 13/2$,

$$\mu_\perp = 4/15(2a_{1/2}^2 + \sqrt{7}a_{11/2}a_{13/2}) \quad (11)$$

and

$$\mu = \sqrt{\mu_\parallel{}^2 + \mu_\perp{}^2}. \quad (12)$$

TABLE 2

ENERGIES, EIGENFUNCTIONS, AND MAGNETIC MOMENTS

$J = 8 \longrightarrow 2\Gamma_1$ (singlet) + Γ_2 (singlet) + Γ_3 (singlet) + Γ_4 (singlet) + $3\Gamma_5$ (doublet) + $3\Gamma_6$ (doublet)

(Ho^{+3})

$|\Gamma_1\rangle = |o\rangle = a_6|-6\rangle + a_0|0\rangle + a_6|6\rangle, a_0^2 > 2a_6^2$; $\mu = 0$

x	E	a_0	a_6
±1.0	±252	1.000	0.000
-.8	-227	.999	-.034
-.6	-204	.993	-.086
-.4	-188	.971	-.169
-.2	-184	.907	-.298
0.0	-204	.775	-.447
0.2	8	.836	-.388
0.4	47	.957	-.205
0.6	109	.991	-.095
0.8	179	.999	-.035

$|\Gamma_3\rangle^* \equiv |3^s\rangle = \frac{1}{\sqrt{2}}[|-3\rangle + |3\rangle]$; $\mu = 0$ for $x \neq \pm 1$

x	E
±1	±21
0	208.5

Energy is linear with x

$|\Gamma_4\rangle^* \equiv |3^a\rangle = \frac{1}{\sqrt{2}}[|-3\rangle - |3\rangle]$; $\mu = 0$ for $x \neq \pm 1$

x	E
±1	±21
0	-22.5

Energy is linear with x

* When $x = \pm 1$ Γ_3 and Γ_4 converge to a doublet whose eigenfunctions are $|\pm 3\rangle$ and the associated moment is 0.375.

$|\Gamma_5\rangle \equiv |d\rangle = a_4|\mp 4\rangle + a_2|\pm 2\rangle + a_8|\pm 8\rangle, a_4^2 > a_2^2, a_8^2$

x	E	μ	a_2	a_4	a_8
±1.0	±168	0.500	0.000	1.000	0.000
-0.8	162	0.495	0.086	0.996	0.001
-0.6	160	0.474	0.188	0.982	0.005
-0.4	165	0.432	0.300	0.954	0.016
-0.2	176	0.371	0.410	0.911	0.044
0.0	193	0.284	0.506	0.853	0.127
0.2	133	0.029	0.535	0.737	-0.413
0.4	-40	0.229	-0.600	0.799	0.033
0.6	-64	0.429	-0.309	0.951	0.009
0.8	-111	0.492	-0.106	0.994	0.001

$|\Gamma_6\rangle \equiv |e\rangle = a_5|\mp 5\rangle + a_1|\pm 1\rangle + a_7|\pm 7\rangle, a_5^2 > a_1^2, a_7^2$

x	E	μ	a_1	a_5	a_7
±1.0	±273	0.625	0.000	1.000	0.000
-0.8	232	0.624	0.045	0.999	0.002
-0.6	194	0.616	0.106	0.994	0.010
-0.4	159	0.597	0.190	0.980	0.024
-0.2	131	0.552	0.305	0.951	0.046
0.0	112	0.467	0.446	0.892	0.074
0.2	66	0.273	0.666	0.738	0.114
0.4	-92	0.458	-0.355	0.909	-0.220
0.6	-144	0.575	-0.165	0.976	0.140
0.8	-206	0.623	-0.052	0.999	0.005

$|\Gamma_7\rangle \equiv |a\rangle = a_5|\mp 5\rangle + a_1|\pm 1\rangle + a_7|\pm 7\rangle, a_5^2 > a_1^2, a_7^2$

x	E	μ	a_1	a_5	a_7
±1.0	±217	0.125	1.000	0.000	0.000
-0.8	-192	0.125	0.998	-0.045	-0.041
-0.6	-170	0.127	0.988	-0.104	-0.117
-0.4	-157	0.164	0.942	-0.176	-0.287
-0.2	-163	0.375	0.759	-0.213	-0.616
0.0	-104	0.211	0.738	-0.414	0.534
0.2	- 80	0.112	0.671	-0.658	0.342
0.4	64	0.024	0.913	0.388	0.127
0.6	104	0.112	0.985	0.155	0.082
0.8	158	0.124	0.998	0.052	0.035

$|\Gamma_5\rangle \equiv |b\rangle = a_8|\mp 8\rangle + a_2|\mp 2\rangle + a_4|\pm 4\rangle, a_2^2 > a_4^2, a_8^2$

x	E	μ	a_2	a_4	a_8
±1.0	±119	0.250	1.000	0.000	0.000
-0.8	- 97	0.245	0.996	-0.086	0.026
-0.6	- 78	0.230	0.978	-0.187	0.089
-0.4	- 60	0.370	0.833	-0.270	0.483
-0.2	- 65	0.169	0.895	-0.392	-0.212
0.0	- 64	0.077	0.862	-0.494	-0.115
0.2	- 45	0.027	0.788	-0.612	-0.070
0.4	97	0.013	0.794	0.600	-0.096
0.6	86	0.180	0.950	0.309	-0.049
0.8	98	0.242	0.994	0.106	-0.021

$|\Gamma_1\rangle^* \equiv |f\rangle = a_6|-6\rangle + a_0|0\rangle + a_6|6\rangle, 2a_6^2 > a_0^2$, $\mu = 0$ for $x \neq \pm 1$

x	E	a_0	a_6
±1.0	±273		
-0.8	204	0.048	0.700
-0.6	138	0.121	0.702
-0.4	78	0.239	0.687
-0.2	30	0.421	0.641
0.0	6	0.632	0.548
0.2	-171	-0.548	0.591
0.4	-175	-0.290	0.677
0.6	-201	-0.134	0.701
0.8	-235	-0.050	0.706

TABLE 2—*continued*

$|\Gamma_2\rangle^* \equiv |6^0\rangle = \frac{1}{\sqrt{2}}[|-6\rangle - |6\rangle]; \quad \mu = 0 \text{ for } x \neq \pm 1$

x	E
±1	±273
0	- 78

Energy is linear with x

*When $x = \pm 1$, Γ_1 and Γ_2 converge to a doublet whose eigenfunctions are $|\pm 6\rangle$ and the associated moment is 0.75.

$|\Gamma_6\rangle \equiv |g\rangle = a_5|\mp 5\rangle + a_1|\pm 1\rangle + a_7|\pm 7\rangle, a_7^2 > a_1^2, a_5^2$

x	E	μ	a_1	a_5	a_7
±1.0	±91	0.875	0.000	0.000	1.000
-0.8	39	0.874	0.040	0.004	0.999
-0.6	-11	0.864	0.116	-0.022	0.993
-0.4	-57	0.808	0.278	-0.077	0.958
-0.2	-90	0.552	0.576	-0.223	0.787
0.0	-197	0.632	-0.507	-0.184	0.842
0.2	-166	0.760	-0.327	0.152	0.933
0.4	-144	0.808	-0.201	0.156	0.967
0.6	-123	0.838	-0.058	-0.152	0.987
0.8	-107	0.874	-0.035	-0.007	0.999

$|\Gamma_5\rangle \equiv |h\rangle = a_8|\mp 8\rangle + a_2|\mp 2\rangle + a_4|\pm 4\rangle, a_8^2 > a_2^2, a_4^2$

x	E	μ	a_2	a_4	a_8
±1.0	±364	1.000	0.000	0.000	1.000
-0.8	-271	1.000	-0.026	0.001	1.000
-0.6	-178	0.994	-0.088	0.012	0.996
-0.4	-90	0.812	-0.464	0.131	0.876
-0.2	14	0.953	0.176	-0.127	0.976
0.0	105	0.957	0.035	-0.167	0.985
0.2	162	0.806	0.305	0.288	0.908
0.4	209	0.992	0.096	0.032	0.995
0.6	260	0.998	0.049	0.007	0.999
0.8	312	1.000	0.021	0.001	1.000

$J = 15/2 \longrightarrow 3\,\Gamma_7\,(\text{doublet}) + 2\,\Gamma_8\,(\text{doublet}) + 3\,\Gamma_9\,(\text{doublet})$

(Dy^{+3}, Er^{+3})

$|\Gamma_7\rangle \equiv |a\rangle = a_{\frac{13}{2}}|\mp\tfrac{13}{2}\rangle + a_{\frac{1}{2}}|\mp\tfrac{1}{2}\rangle + a_{\frac{11}{2}}|\pm\tfrac{11}{2}\rangle, a_{\frac{1}{2}}^2 > a_{\frac{11}{2}}^2, a_{\frac{13}{2}}^2$

x	E	$\mu_{\|\|}$	$\mu_\perp$	μ	$a_{1/2}$	$a_{11/2}$	$a_{13/2}$
∓1.0	∓189	0.067	0.533	0.538	1.000	0.000	0.000
-0.8	-167	0.067	0.533	0.537	0.999	-0.032	-0.033
-0.6	-147	0.068	0.531	0.535	0.992	-0.082	-0.093
-0.4	-131	0.083	0.519	0.526	0.963	-0.161	-0.215
-0.2	-127	0.187	0.466	0.502	0.843	-0.262	-0.468
0	- 89	0.137	0.120	0.190	-0.509	-0.560	0.653
0.2	8	0.064	0.467	0.471	0.865	0.455	0.209
0.4	41	0.048	0.520	0.523	0.968	0.208	0.142
0.6	87	0.065	0.531	0.535	0.993	0.092	0.076
0.8	137	0.067	0.533	0.537	0.999	0.034	0.031

$|\Gamma_9\rangle \equiv |b\rangle = a_{\frac{9}{2}}|\mp\tfrac{9}{2}\rangle + a_{\frac{3}{2}}|\pm\tfrac{3}{2}\rangle + a_{\frac{15}{2}}|\pm\tfrac{15}{2}\rangle, a_{\frac{3}{2}}^2 > a_{\frac{9}{2}}^2, a_{\frac{15}{2}}^2$

x	E	μ	$a_{\frac{3}{2}}$	$a_{\frac{9}{2}}$	$a_{\frac{15}{2}}$
∓1.0	±129	0.200	1.000	0.000	0.000
-0.8	-109	0.199	0.998	-0.049	0.037
-0.6	- 90	0.206	0.983	-0.117	0.144
-0.4	- 84	0.477	-0.775	0.162	0.610
-0.2	- 69	0.145	0.923	-0.329	-0.198
0.0	- 66	0.025	0.858	-0.483	-0.117
0.2	- 50	0.186	0.714	-0.698	-0.065
0.4	53	0.087	0.916	0.389	-0.102
0.6	72	0.182	0.985	0.163	-0.059
0.8	99	0.198	0.998	0.056	-0.027

$|\Gamma_8\rangle \equiv |c\rangle = a_{\frac{7}{2}}|\mp\tfrac{7}{2}\rangle + a_{\frac{5}{2}}|\pm\tfrac{5}{2}\rangle, a_{\frac{5}{2}}^2 > a_{\frac{7}{2}}^2$

x	E	μ	$\mu_{\|\|}$	$\mu_\perp$	$a_{5/2}$	$a_{7/2}$		
∓1.0	∓25	0.333	0.333	0	1.000	0.000	0.467	0.467	467
-0.8	-12	0.346	0.318	0.138	0.990	-0.140	0.481	0.471	100
-0.6	- 5	0.384	0.264	-0.279	0.955	-0.295	0.485	0.397	105
-0.4	- 5	0.427	0.183	-0.386	0.901	-0.433	0.317	0.499	135
-0.2	- 8	0.459	0.103	-0.448	0.844	-0.536	0.256	0.506	129
0	-15	0.479	0.038	-0.477	0.794	-0.608	0.171	0.507	147
0.2	-17	0.496	0.039	-0.493	0.732	-0.681	0.095	0.502	107
0.4	72	0.490	0.034	0.478	0.791	0.611	0.168	0.507	- 24
0.6	45	0.417	0.205	0.363	0.916	0.400	0.338	0.496	- 39
0.8	30	0.351	0.312	0.160	0.986	0.164	0.445	0.473	- 66

x			$-\mu_\perp$	$a_{7/2}$	$a_{5/2}$	$\mu_{\|\|}$	μ	E

$|\Gamma_8\rangle \equiv |d\rangle = a_{\frac{7}{2}}|\mp\tfrac{7}{2}\rangle - a_{\frac{5}{2}}|\pm\tfrac{5}{2}\rangle, a_{\frac{7}{2}}^2 > a_{\frac{5}{2}}^2$

$|\Gamma_9\rangle \equiv |e\rangle = a_{\frac{15}{2}}|\mp\tfrac{15}{2}\rangle + a_{\frac{3}{2}}|\mp\tfrac{3}{2}\rangle + a_{\frac{9}{2}}|\pm\tfrac{9}{2}\rangle, a_{\frac{9}{2}}^2 > a_{\frac{3}{2}}^2, a_{\frac{15}{2}}^2$

x	E	μ	$a_{\frac{3}{2}}$	$a_{\frac{9}{2}}$	$a_{\frac{15}{2}}$
±1.0	±201	0.600	0.000	1.000	0.000
-0.8	173	0.598	0.049	0.999	0.000
-0.6	148	0.589	0.118	0.993	0.003
-0.4	125	0.563	0.214	0.977	0.012
-0.2	108	0.502	0.344	0.938	0.044
0.0	100	0.305	0.496	0.832	0.247
0.2	60	0.169	0.675	0.709	-0.205
0.4	-63	0.478	-0.389	0.921	0.020
0.6	-102	0.579	-0.163	0.987	0.004
0.8	-150	0.598	-0.056	0.998	0.001

$|\Gamma_7\rangle \equiv |f\rangle = a_{\frac{11}{2}}|\mp\tfrac{11}{2}\rangle + a_{\frac{1}{2}}|\pm\tfrac{1}{2}\rangle + a_{\frac{13}{2}}|\pm\tfrac{13}{2}\rangle, a_{\frac{11}{2}}^2 > a_{\frac{1}{2}}^2, a_{\frac{13}{2}}^2$

x	E	$\mu_{\|\|}$	$\mu_\perp$	μ	$a_{1/2}$	$a_{11/2}$	$a_{13/2}$
∓1.0	±221	0.733	0	0.733	0.000	1.000	0.000
-0.8	169	0.733	0.002	0.733	0.032	0.999	0.001
-0.6	119	0.729	0.012	0.728	0.083	0.996	0.010
-0.4	71	0.707	0.041	0.709	0.173	0.984	0.036
-0.2	29	0.624	0.126	0.637	0.344	0.934	0.096
0	5	0.380	0.299	0.484	0.612	0.769	0.182
0.2	-92	0.294	-0.221	0.367	-0.317	0.821	-0.473
0.4	-121	0.458	0.270	0.531	-0.247	0.893	0.376
0.6	-150	0.725	0.025	0.725	-0.095	0.995	0.028
0.8	-185	0.732	0.003	0.732	-0.034	0.999	0.002

TABLE 2—*continued*

$|\Gamma_7\rangle \equiv |g\rangle = a_{\frac{11}{2}}|\mp\tfrac{11}{2}\rangle + a_{\frac{1}{2}}|\pm\tfrac{1}{2}\rangle + a_{\frac{13}{2}}|\pm\tfrac{13}{2}\rangle, a_{\frac{13}{2}}^2 > a_{\frac{1}{2}}^2, a_{\frac{11}{2}}^2$

x	E	$\mu_{\|\|}$	$\mu_\perp$	μ	$a_{1/2}$	$a_{11/2}$	$a_{13/2}$
∓1.0	± 91	0.867	0	0.867	0.000	0.000	1.000
-0.8	50	0.866	-0.02	0.866	0.033	-0.003	0.999
-0.6	9	0.859	-0.009	0.859	0.091	-0.018	0.996
-0.4	- 29	0.824	-0.027	0.825	0.206	-0.072	0.976
-0.2	- 62	0.637	-0.059	0.640	0.412	-0.241	0.878
0	-147	0.423	0.355	0.552	-0.604	0.307	0.735
0.2	-125	0.558	0.287	0.628	-0.387	0.343	0.855
0.4	-108	0.610	-0.257	0.662	-0.049	-0.399	0.916
0.6	-102	0.860	-0.022	0.861	-0.074	-0.035	0.997
0.8	- 96	0.866	-0.002	0.866	-0.050	-0.003	0.999

$|\Gamma_9\rangle \equiv |h\rangle = a_{\frac{9}{2}}|\mp\tfrac{9}{2}\rangle + a_{\frac{3}{2}}|\pm\tfrac{3}{2}\rangle + a_{\frac{15}{2}}|\pm\tfrac{15}{2}\rangle, a_{\frac{15}{2}}^2 > a_{\frac{3}{2}}^2, a_{\frac{9}{2}}^2$

x	E	μ	$a_{\frac{3}{2}}$	$a_{\frac{9}{2}}$	$a_{\frac{15}{2}}$
∓1.0	∓273	1.000	0.000	0.000	1.000
-0.8	-206	0.999	-0.037	0.001	0.999
-0.6	-139	0.983	-0.144	0.014	0.990
-0.4	- 62	0.686	0.594	-0.139	0.792
-0.2	0	0.958	0.171	-0.109	0.979
0.0	65	0.881	-0.022	-0.273	0.962
0.2	109	0.955	0.189	0.103	0.977
0.4	149	0.991	0.102	0.022	0.995
0.6	190	0.997	0.059	0.006	0.998
0.8	231	0.999	0.027	0.001	1.000

$J=6 \rightarrow 2\Gamma_1(\text{singlet}) + \Gamma_2(\text{singlet}) + \Gamma_3(\text{singlet}) + \Gamma_4(\text{singlet})$
$(Tb^{3+}, Tm^{3+}) \quad + 2\Gamma_5(\text{doublet}) + 2\Gamma_6(\text{doublet})$

$|\Gamma_1\rangle \equiv |0\rangle = a_6|-6\rangle + a_0|0\rangle + a_6|6\rangle, a_0^2 > 2a_6^2 \quad \mu = 0$

x	E	a_0	a_6
∓1.0	∓84	1.000	0.000
-0.8	-78	0.725	-0.487
-0.6	-70	0.924	-0.270
-0.4	-62	0.948	-0.225
-0.2	-54	0.956	-0.207
0.0	-46	0.960	-0.198
0.2	-20	0.964	-0.189
0.4	7	0.969	-0.175
0.6	33	0.976	-0.153
0.8	59	0.988	-0.110

$|\Gamma_6\rangle \equiv |a\rangle = a_5|\mp 5\rangle + a_1|\pm 1\rangle, a_1^2 > a_5^2$

x	E	μ	a_1	a_5		
±1.0	∓64	0.167	1.000	0.000	0.833	±66
-0.8	-55	0.164	0.999	-0.053	0.831	42
-0.6	-48	0.142	0.988	-0.157	0.809	19
-0.4	-44	0.019	0.923	-0.385	0.685	- 0
-0.2	- 9	0.309	0.724	0.690	0.357	- 1
0.0	- 6	0.055	0.882	0.471	0.612	-69
0.2	4	0.062	0.946	0.323	0.729	-64
0.4	17	0.126	0.980	0.201	0.793	-63
0.6	32	0.154	0.994	0.111	0.821	-63
0.8	47	0.165	0.999	0.047	0.831	-64

x	a_5	a_1	μ	E

$|\Gamma_6\rangle \equiv |e\rangle = a_5|\mp 5\rangle - a_1|\pm 1\rangle, a_5^2 > a_1^2$

$|\Gamma_5\rangle \equiv |b\rangle = a_2|\mp 2\rangle + a_4|\pm 4\rangle, a_2^2 > a_4^2$

x	E	μ	a_2	a_4		
±1.0	∓11.0	0.333	1.000	0.000	0.667	±96
-0.8	- 5.0	0.326	0.996	-0.084	0.660	79
-0.6	- 1.0	0.284	0.975	-0.222	0.618	64
-0.4	- 1.2	0.149	0.903	-0.429	0.483	53
-0.2	- 8.1	0.077	0.768	-0.641	0.296	49
0.0	50.8	0.069	0.773	0.634	0.264	-21
0.2	36.0	0.084	0.867	0.499	0.417	-29
0.4	25.2	0.219	0.941	0.338	0.553	-41
0.6	18.1	0.297	0.982	0.190	0.631	-57
0.8	13.8	0.327	0.997	0.079	0.661	-76

x	a_4	a_2	μ	E

$|\Gamma_5\rangle \equiv |d\rangle = a_4|\mp 4\rangle - a_2|\pm 2\rangle, a_4^2 > a_2^2$

$|\Gamma_3\rangle^* \equiv |3^a\rangle = \frac{1}{\sqrt{2}}[\,|-3\rangle + |3\rangle\,]; \mu = 0 \text{ for } x \neq \pm 1$

x	E
±1	±54
0	81.5

Energy is linear with x

$|\Gamma_4\rangle^* \equiv |3^a\rangle = \frac{1}{\sqrt{2}}[\,|-3\rangle - |3\rangle\,]; \mu = 0 \text{ for } x \neq \pm 1$

x	E
∓1	±54
0	4.5

Energy is linear with x

*When x = ±1 Γ_3 and Γ_4 converge to a doublet whose eigenfunctions are $|\pm 3\rangle$ and the associated moment is 0.50.

$|\Gamma_1\rangle^* \equiv |f\rangle = a_6|-6\rangle + a_6|0\rangle + a_6|6\rangle, 2a_6^2 > a_0^2,$
$\mu = 0 \text{ for } x \neq \pm 1$

x	E	a_0	a_6
∓1	∓99		
-0.8	-71	0.690	0.512
-0.6	-47	0.383	0.653
-0.4	-22	0.319	0.670
-0.2	3	0.293	0.676
0.0	28	0.279	0.679
0.2	42	0.267	0.682
0.4	56	0.248	0.685
0.6	70	0.217	0.690
0.8	84	0.155	0.699

$|\Gamma_2\rangle^* \equiv |6^a\rangle = \frac{1}{\sqrt{2}}[\,|-6\rangle - |6\rangle\,]; \mu = 0 \text{ for } x \neq \pm 1$

x	E
∓1	∓99
0	22

Energy is linear with x

*When x = ±1, Γ_1 and Γ_2 converge to a doublet whose eigenfunctions are $|\pm 6\rangle$ and the associate moment is 1.00.

TABLE 2—*continued*

$J = \frac{9}{2} \rightarrow \Gamma_7$ (doublet) + 2 Γ_8 (doublet) + 2 Γ_9 (doublet)

(Nd^{3+})

$|\Gamma_7\rangle \equiv |a\rangle = |\pm 1/2\rangle$

$\mu_{\parallel} = 0.111 \quad \mu_{\perp} = 0.556 \quad \mu = 0.567$

x	E
±1	±25.2
0	-16

E is linear with x

$|\Gamma_9\rangle \equiv |b\rangle = a_{\frac{3}{2}} |\mp \tfrac{3}{2}\rangle + a_{\frac{9}{2}} |\pm \tfrac{9}{2}\rangle, a^2_{\frac{3}{2}} > a^2_{\frac{9}{2}}$

x	E	μ	$a_{\frac{3}{2}}$	$a_{\frac{9}{2}}$		
±1.0	±4.2	0.333	1.000	0.000	1.000	±25.2
-0.8	-0.6	0.309	0.991	0.136	0.975	-19.3
-0.6	3.8	0.220	0.956	0.292	0.887	-14.3
-0.4	9.2	0.081	0.900	0.435	0.748	-10.1
-0.2	15.3	0.062	0.839	0.544	0.605	- 6.8
0.0	22.0	0.179	0.785	0.620	0.488	- 4.0
0.2	20.2	0.314	0.717	0.697	0.353	0.1
0.4	3.4	0.132	0.807	-0.591	0.535	19.2
0.6	5.3	0.141	0.925	-0.380	0.808	19.6
0.8	5.4	0.310	0.988	-0.156	0.968	21.8

x	$a^2_{\frac{9}{2}}$	$a^2_{\frac{3}{2}}$	μ	E

$|\Gamma_9\rangle \equiv |e\rangle = a_{\frac{9}{2}} |\mp \tfrac{9}{2}\rangle - a_{\frac{3}{2}} |\pm \tfrac{3}{2}\rangle, a^2_{\frac{9}{2}} > a^2_{\frac{3}{2}}$

$|\Gamma_8\rangle \equiv |C\rangle = a_{\frac{5}{2}} |\mp \tfrac{5}{2}\rangle + a_{\frac{7}{2}} |\pm \tfrac{7}{2}\rangle, a^2_{\frac{5}{2}} > a^2_{\frac{7}{2}}$

x	E	μ	$\mu_{\parallel}$	$\mu_{\perp}$	$a^2_{\frac{5}{2}}$	$a^2_{\frac{7}{2}}$			
±1.0	±23.8	0.556	0.556	0	1.000	0.000	0.778	0.778	±30.8
-0.8	25.7	0.434	0.117	0.418	0.819	0.576	0.339	0.538	17.5
-0.6	25.9	0.454	0.311	0.344	0.904	0.428	0.533	0.635	6.0
-0.4	26.4	0.476	0.353	0.319	0.921	0.390	0.575	0.698	- 5.8
-0.2	26.9	0.481	0.371	0.307	0.928	0.372	0.593	0.668	-17.6
0.0	27.5	0.485	0.380	0.300	0.932	0.363	0.603	0.673	-29.5
0.2	17.1	0.488	0.389	0.294	0.936	0.353	0.612	0.678	-29.6
0.4	6.6	0.493	0.403	0.283	0.941	0.338	0.625	0.686	-29.7
0.6	- 3.8	0.501	0.427	0.263	0.950	0.311	0.649	0.700	-29.8
0.8	-14.1	0.519	0.473	0.214	0.969	0.249	0.695	0.728	-30.0

x	$-\mu_{\perp}$	$a^2_{\frac{7}{2}}$	$a^2_{\frac{5}{2}}$	$\mu_{\parallel}$	μ	E

$|\Gamma_8\rangle \equiv |d\rangle = a_{\frac{7}{2}} |\mp \tfrac{7}{2}\rangle - a_{\frac{5}{2}} |\pm \tfrac{5}{2}\rangle, a^2_{\frac{7}{2}} > a^2_{\frac{5}{2}}$

$J = 4 \rightarrow \Gamma_1$ (singlet) + Γ_3 (singlet) + Γ_4 (singlet)

(Pr^{3+}, Pm^{3+}) + 2 Γ_5 (doublet) + Γ_6 (doublet)

$|\Gamma_1\rangle \equiv |0\rangle = |0\rangle \qquad \Gamma_6 = |a\rangle = |\pm 1\rangle$

$\mu = 0 \qquad \mu = 0.25$

E is a linear function of x

x	E
±1	±18
0	-20

E is a linear function of x

x	E
±1	±9
0	1

$|\Gamma_5\rangle \equiv |b\rangle = a_2 |\mp 2\rangle + a_4 |\pm 4\rangle, a^2_2 > a^2_4$

x	E	μ	a_2	a_4		
±1.0	±11.0	0.500	1.000	0.000	1.000	±14.0
-0.6	13.6	0.478	0.993	0.121	0.978	-10.8
-0.6	16.8	0.414	0.971	0.239	0.914	- 8.2
-0.4	20.8	0.324	0.940	0.342	0.824	- 6.4
-0.2	25.3	0.230	0.906	0.424	0.730	- 5.1
0.0	30.1	0.145	0.873	0.487	0.645	- 4.1
0.2	23.3	0.031	0.829	0.559	0.531	- 1.9
0.4	17.1	0.216	0.723	0.691	0.284	- 0.3
0.6	- 0.9	0.168	0.882	-0.471	0.668	13.1
0.8	- 4.9	0.457	0.985	-0.170	0.957	12.5

x	a_4	a_2	μ	E

$|\Gamma_5\rangle \equiv |d\rangle = a_4 |\mp 4\rangle - a_2 |\pm 2\rangle, a^2_4 > a^2_2$

$|\Gamma_3\rangle^* \equiv |3^a\rangle = \frac{1}{\sqrt{2}} [|-3\rangle + |3\rangle]; \mu = 0$ for $x \neq \pm 1$

x	E
±1	±21
0	2.25

Energy is linear with x

$|\Gamma_4\rangle^* \equiv |3^a\rangle = \frac{1}{\sqrt{2}} [|-3\rangle - |3\rangle]; \mu = 0$ for $x \neq \pm 1$

x	E
±1	±21
0	-36.25

Energy is linear with x

When $x = \pm 1$ Γ_3 and Γ_4 converge to a doublet whose eigenfunctions are $|\pm 3\rangle$ and the associated moment is 0.75.

$J = \frac{7}{2} \rightarrow \Gamma_7$ (doublet) + 2 Γ_8 (doublet) + Γ_9 (doublet)

(Yb^{3+})

$|\Gamma_7\rangle \equiv |a\rangle = |\pm \tfrac{1}{2}\rangle$

$\mu_{\parallel} = 0.143 \quad \mu_{\perp} = 0.571 \quad \mu = 0.589$

x	E
±1	±9
0	-5

E is a linear function of x

$|\Gamma_9\rangle \equiv |b\rangle = |\pm \tfrac{3}{2}\rangle$

$\mu = 0.429$

x	E
±1	±3
0	0

E is a linear function of x

TABLE 2—*continued*

$|\Gamma_8\rangle \equiv |c\rangle = a_{\frac{5}{2}}|\mp\tfrac{5}{2}\rangle + a_{\frac{7}{2}}|\pm\tfrac{7}{2}\rangle,\ a_{\frac{5}{2}}^2 > a_{\frac{7}{2}}^2$

x	E	μ	$\mu_{\parallel}$	$\mu_{\perp}$	$a_{5/2}$	$a_{7/2}$			
∓1.0	±13.0	0.714	0.714	0	1.000	0.000	1.000	1.000	∓7.0
-0.8	9.5	0.702	0.698	0.073	0.995	0.097	0.984	0.987	-5.5
-0.6	6.6	0.622	0.590	0.196	0.963	0.269	0.876	0.898	-4.6
-0.4	4.9	0.416	0.243	0.338	0.851	0.524	0.529	0.627	-4.9
-0.2	- 6.8	0.386	0.084	-0.377	0.731	-0.682	0.202	0.428	4.8
0	- 9.9	0.395	0.184	-0.349	0.831	-0.556	0.470	0.585	5.9
0.2	- 9.5	0.480	0.374	-0.302	0.895	-0.446	0.660	0.725	5.1
0.4	- 9.7	0.588	0.542	-0.227	0.948	-0.317	0.828	0.858	4.9
0.6	-10.4	0.666	0.652	-0.142	0.982	-0.191	0.938	0.948	5.2
0.8	-11.5	0.705	0.702	-0.063	0.996	-0.084	0.988	0.990	5.9

x	$-\mu_{\perp}$	$a_{7/2}$	$a_{5/2}$	$\mu_{\parallel}$	μ	E

$|\Gamma_8\rangle \equiv |d\rangle = a_{\frac{7}{2}}|\mp\tfrac{7}{2}\rangle - a_{\frac{5}{2}}|\pm\tfrac{5}{2}\rangle,\ a_{\frac{7}{2}}^2 > a_{\frac{5}{2}}^2$

$J = \frac{5}{2} \rightarrow \Gamma_7(\text{doublet}) + \Gamma_8(\text{doublet}) + \Gamma_9(\text{doublet})$

(Ce^{3+}, Sm^{3+})

No sixth order influence	X=+1	X=−1
$\|\Gamma_7\rangle = \|a\rangle = \|\pm\frac{1}{2}\rangle$		
$\mu_{\parallel} = 0.7$ $\mu_{\perp} = 0.6$ $\mu = 0.632$	E=+2	−2
$\|\Gamma_9\rangle \equiv \|b\rangle = \|\pm 3/2\rangle$		
$\mu_{\parallel} = 0.6$ $\mu_{\perp} = 0$	E=−3	+3
$\|\Gamma_8\rangle = \|c\rangle = \|\pm 5/2\rangle$		
$\mu_{\parallel} = 1$ $\mu_{\perp} = 0$	E=+1	−1

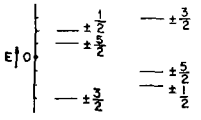

Explanation of Symbols in Table

x is a parameter giving the relative importance of the fourth- and sixth-order terms. E is the energy in units of the parameter W. (For definitions of x and W see Eq. 13.) a_M are the normalized coefficients in the eigenfunction $|\Gamma_i\rangle = \sum_{m=-J}^{J} a_{iM}|M\rangle$. $\mu_{\parallel}$ and $\mu_{\perp}$ are magnetic moments (divided by $gJ\ \mu_B$) along directions parallel and perpendicular to the c axis, respectively. $\mu = \sqrt{\mu_{\parallel}^2 + \mu_{\perp}^2}$.

The table has been constructed for the group D_6 (= 622). Concerning the number of terms and their degeneracies this table is also valid for other hexagonal point groups (*23*).

The moments given in Eqs. (7), (8), (10), (11), and (12) and in Table 2 are reduced moments. To obtain the moment in Bohr magnetons per ion the reduced moment is multiplied by gJ.

D. Other Details

For calculations the Hamiltonian was used in the form

$$\mathcal{H} = W\left[x\frac{O_4}{F_4} + (1-|x|)\frac{O_6}{F_6}\right]. \qquad (13)$$

$O_4 = O_4^0, O_6 = O_6^0 + \frac{77}{8}O_6^6, F_4 = 60$ and $F_6 - 1260$ for $J = 7/2$ and 4, 2520 for $J = 9/2$, 7560 for $J = 6$ and 13860 for $J = 15/2$ and 8. The parameter $|x| \leqslant 1$ gives the relative importance of the fourth and sixth degree.

$$B_4 F_4 = Wx, \qquad B_6 F_6 = W(1-|x|). \qquad (14)$$

The point charge model coefficients B_4 and B_6 are the sums

$$B_4 = \frac{-e^2}{64}\beta\langle r^4\rangle \sum_j \frac{Z_j}{R_j^5}(35\cos^4\theta_j - 30\cos^2\theta_j + 3) \qquad (15)$$

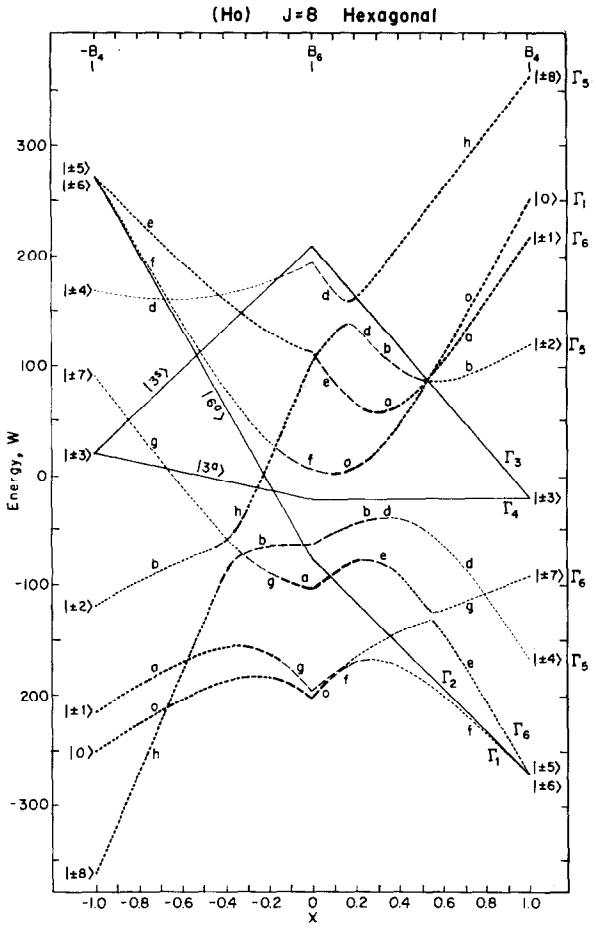

FIG. 1. Energy levels and eigenfunctions of an ion, with a total angular momentum. $J = 8$, as a function of the mixing parameter x.

—— The eigenfunctions of the level do not depend on x.

---- The eigenfunctions are over 80% of the eigenfunctions indicated at $x = \pm 1$.

– – – The eigenfunctions are less than 80% of the eigenfunctions as indicated.

The energy scale is in units of W. When $W > 0$ the order of the levels is as shown. If $W < 0$, the order of the levels is inverted.

and

$$B_6 = \frac{-e^2}{256}\langle r^6\rangle \sum_j \frac{Z_j}{R_j^7} \times (231\cos^6\theta_j - 315\cos^4\theta_j + 105\cos^2\theta_j - 5). \quad (16)$$

In these equations the origin is the center of the magnetic ion. R_j is the distance of the jth ion from the magnetic ion, and θ_j is measured from the z axis, taken in this case to be the hexagonal axis. β and γ are the Stevens (*8*, *18*) multiplicative factors. $e^2 = 1.67097(4)$°K Å.

If the summation is carried out only over the twelve nearest and the six next nearest neighboring ions, one obtains for the $A3$ structure (simple *cph*) with ideal axial ratio (*10*):

$$B_4 = -0.51560\,\beta\langle r^4\rangle \frac{Ze^2}{a^5} \quad (17)$$

and

$$B_6 = 0.263467\,\gamma\langle r^6\rangle \frac{Ze^2}{a^7} \quad (18)$$

assuming all ions have the same charge Z. The lattice constant is denoted by a.

The matrix of Eq. (5) was established using the matrix elements of the equivalent operators tabulated by Hutchings (*16*). Diagonalization was effected by methods which have been described in detail elsewhere (*5*, *6*, *20*).

III. Results and Discussion

Results are summarized in Table 2 and in Figs. 1–15. In the diagrams of the energy levels the nature of the eigenfunctions is indicated. For $x = \pm 1$ the eigenfunctions are written beside the level. When the eigenfunctions of the level do not depend on x, a solid line follows the level. When the eigenfunctions change as a function of x, the line is broken. If the eigenfunctions are 80% or more of that which is indicated for $x = \pm 1$ the dashes are short and dense. When the eigenfunctions are less than 80% the dashes are long.

In Figs. 1–15, it is noted that the levels for $x = 1$ are the inverse of those for $x = -1$. Thus a level with $x = -1$ with certain eigenfunctions must reach at $x = 1$ a level with identical eigenfunctions. For example, in the diagram for $J = \frac{15}{2}$ the level lettered "a" whose eigenfunctions for $x = -1$ are $|\pm 1/2\rangle$ must reach the level whose eigenfunctions are $|\pm 1/2\rangle$ at $x = 1$. In following the levels one keeps to the level which contains more than 50% of the original eigenfunctions. To keep this principle it is necessary to jump from one representation to another which has the *same* symmetry properties. In the example for $J = 15/2$ the level "a" jumps at $x = -0.03$ from $E = -141W$ to $E = -84W$ and continues as the level lettered "g" (originally $|\pm \frac{13}{2}\rangle$). At $x = 0.06$ the level "a" jumps once more, from $E = -88W$ to $E = 2W$, and continues as the level lettered "f" (originally $|\pm \frac{11}{2}\rangle$). In some cases, when a particular representation occurs three times (only for $J = \frac{15}{2}$ and 8) in the neighborhood of a "jumping point" the three components of the eigenfunctions are less than 50% for each component. In such a case we follow the largest component.

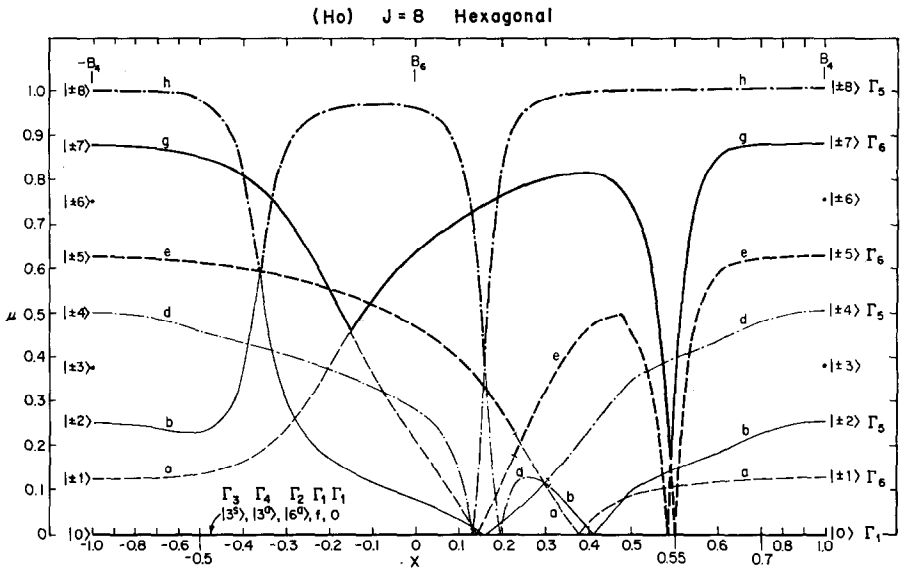

FIG. 2. Permanent (parallel) magnetic moments of the levels in Fig. 1. The two eigenfunctions of the doublet levels have equal and opposite magnetic moments; in the figure only the positive component is shown. (Notice the nonlinear scale of x.)

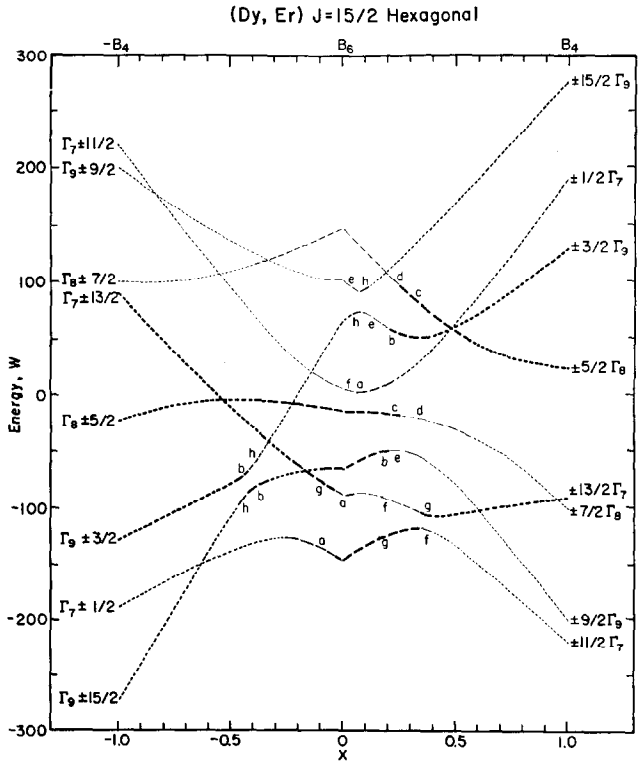

FIG. 3. Data corresponding to that in Fig. 1 for ion with $J = 15/2$.

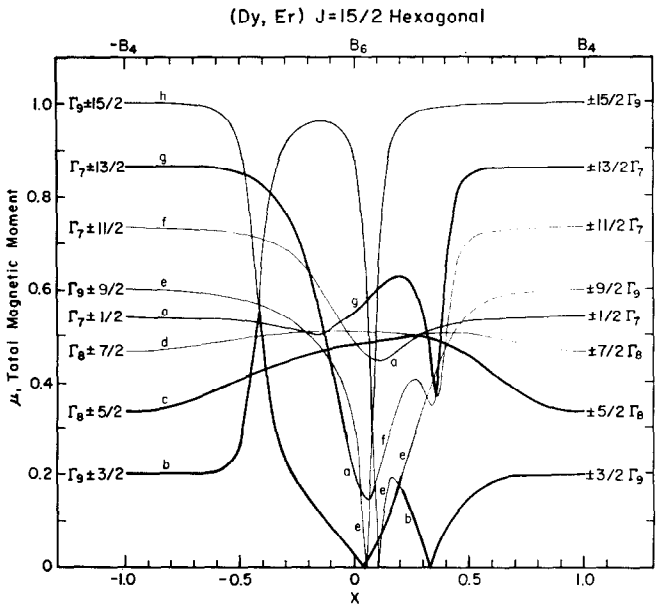

FIG. 4. Total permanent magnetic moment (μ) of the levels of Fig. 3.

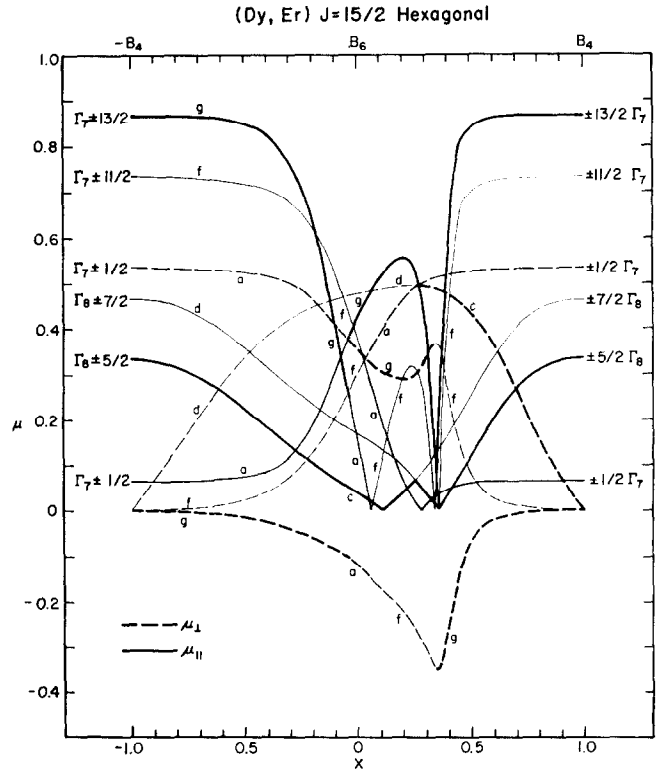

FIG. 5. Permanent parallel ($\mu_\parallel$) and perpendicular ($\mu_\perp$) magnetic moments of the levels of Fig. 3. The two eigenfunctions of a doublet level have one perpendicular component and two parallel components. The two parallel components have equal and opposite magnetic moments. In the figure only the positive component of the parallel moments is shown. The levels *c* and *d* have equal and opposite perpendicular magnetic moments. In the figure only the positive part is shown.

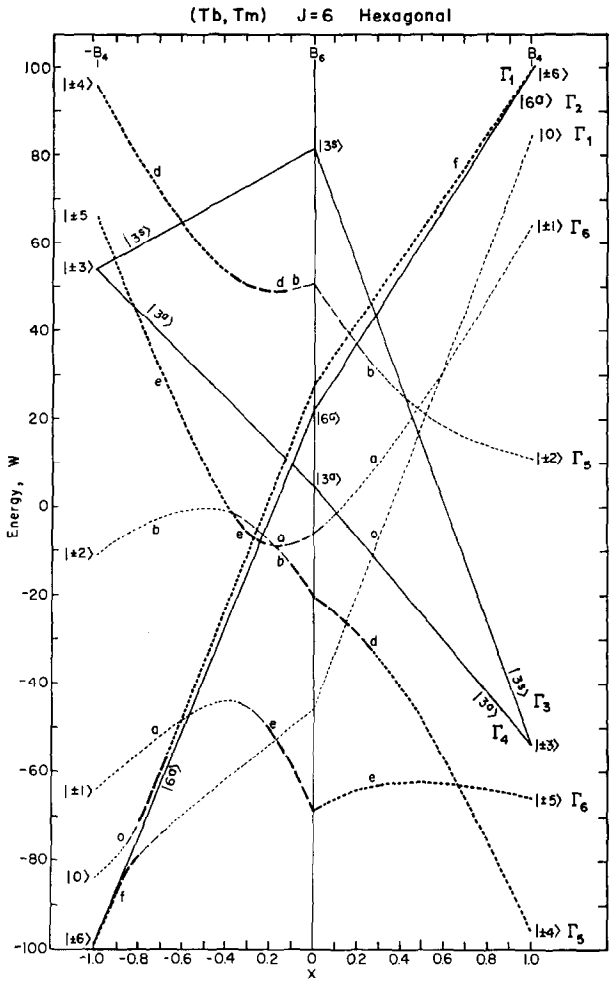

FIG. 6. Data corresponding to that in Fig. 1 for ion with $J = 6$.

Consider the eigenfunctions of the level "a" at $x = 0$ which is close to two "jumping points." In this case between the two "jumping points" the eigenfunctions are $|a\rangle = 0.653\ |\pm\tfrac{13}{2}\rangle - 0.509\ |\pm 1/2\rangle - 0.560\ |\pm\tfrac{11}{2}\rangle$. This level is lettered "a", which originally was $|\pm 1/2\rangle$ because the other two levels (g,f) of the same symetry (Γ_7) are well defined at $x = 0$, which means that these levels (f,g) at $x = 0$ have more than 50% the $|\pm\tfrac{11}{2}\rangle$ and $|\pm\tfrac{13}{2}\rangle$ components respectively. $|f\rangle = 0.769\ \ |\pm\tfrac{11}{2} + 0.612\ |\pm\tfrac{1}{2}\rangle + 0.182\ |\pm\tfrac{13}{2}\rangle$. $|g\rangle = 0.735\ |\pm\tfrac{13}{2}\rangle - 0.604\ |\pm\tfrac{1}{2}\rangle + 0.307\ |\pm\tfrac{11}{2}\rangle$.

This procedure is somewhat complicated but it provides useful information about the eigenfunctions of the level merely by looking at the diagrams. Only for precise knowledge or calculations must one go to the tables.

As noted earlier, the calculations are based on the assumption that $B_6^0/B_6^6 = 8/77$, a ratio which is found experimentally within 10 to 20% for a large number of rare-earth compounds. Some calculations were made with this ratio varying by 10 and 20%. The differences (Figs. 16–19) produced are minor; the order of levels is unchanged and their spacings are only trivially affected. Hence the effect in using the approximate Hamiltonian, instead of the exact one involving the B_6^0, B_6^6 ratio appropriate to the particular compound under investigation, will be to obtain slightly different values for the parameters W and x when the theoretical results obtained in

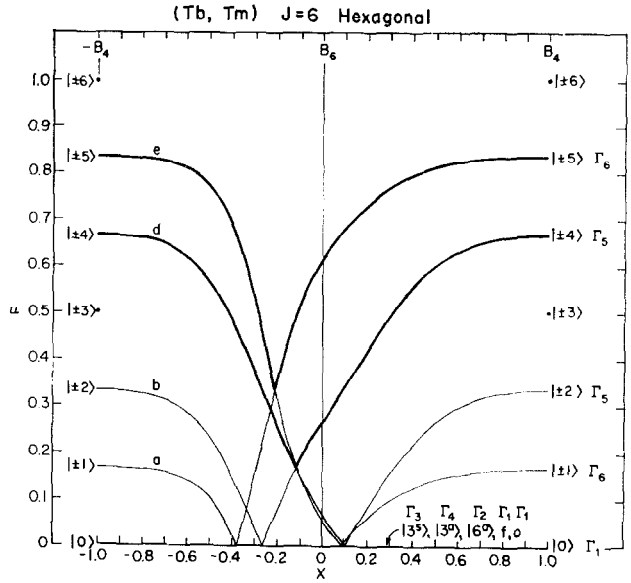

FIG. 7. Data corresponding to that of Fig. 2 for ion with $J = 6$.

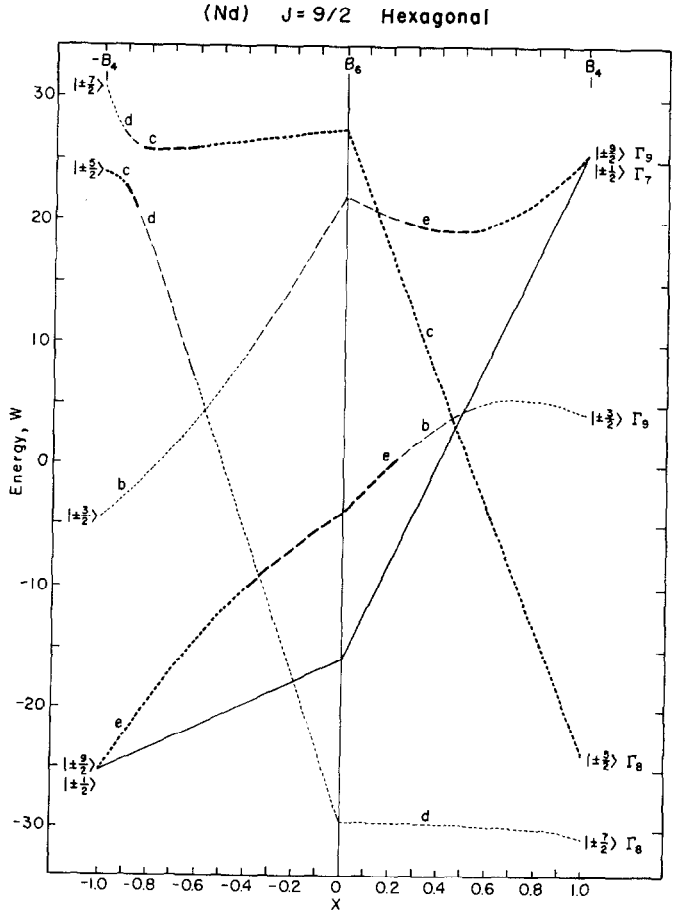

FIG. 8. Data corresponding to that in Fig. 1 for ion with $J = 9/2$.

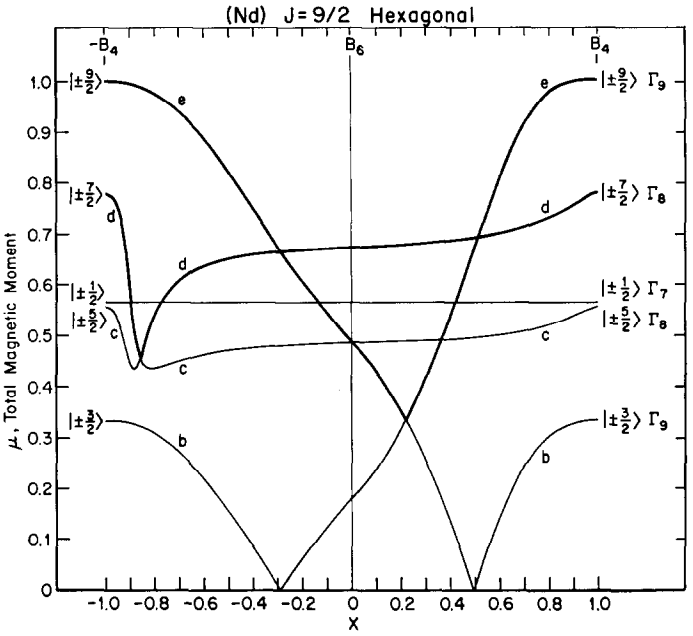

FIG. 9. Data corresponding to that in Fig. 4 for ion with $J = 9/2$.

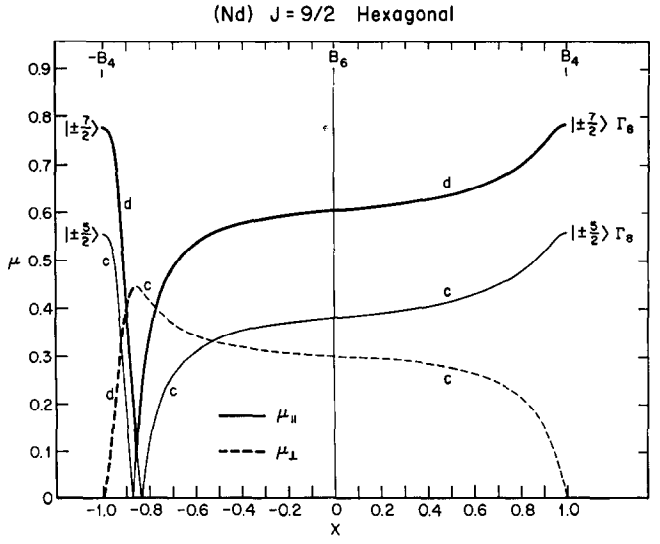

FIG. 10. Data corresponding to that in Fig. 5 for ion with $J = 9/2$.

parametrical form are compared with experiment. The W and x parameters will have less intrinsic significance than would be the case if the exact Hamiltonian were employed. Notwithstanding this limitation the present results would seem to be of very considerable utility in respect to the evaluation of the influence of the crystal field interaction on the bulk magnetic and thermal properties of crystals containing rare-earth ions. Examples of these uses are to be found in recent publications from this

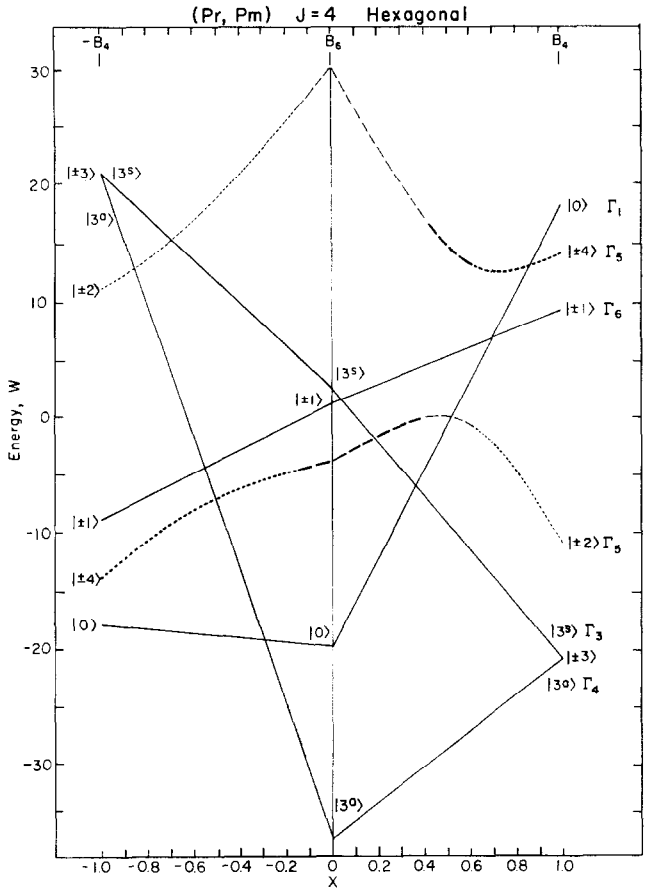

FIG. 11. Data corresponding to that in Fig. 1 for ion with $J = 4$.

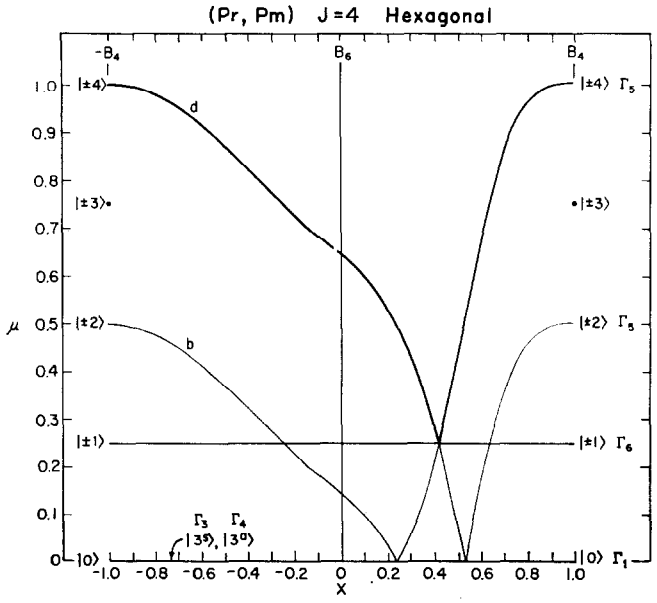

FIG. 12. Data corresponding to that in Fig. 2 for ion with $J = 4$.

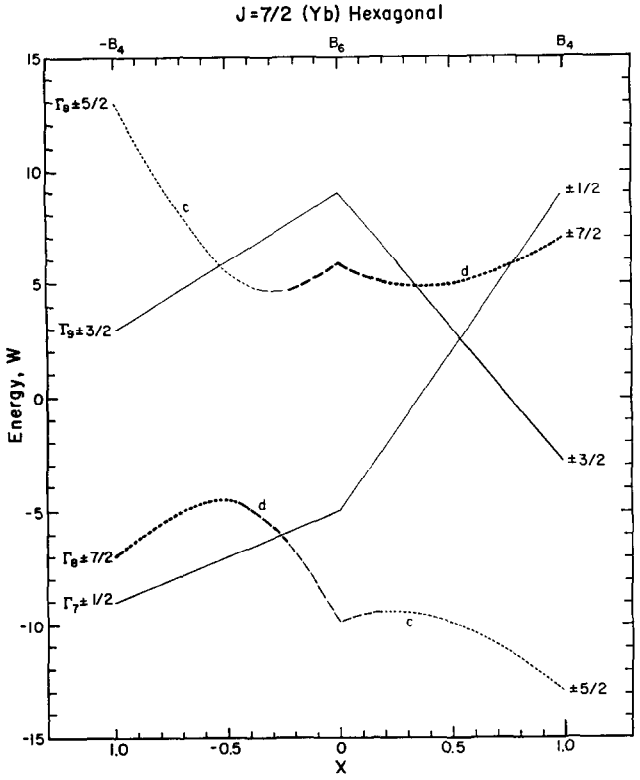

FIG. 13. Data corresponding to that in Fig. 1 for ion with $J = 7/2$.

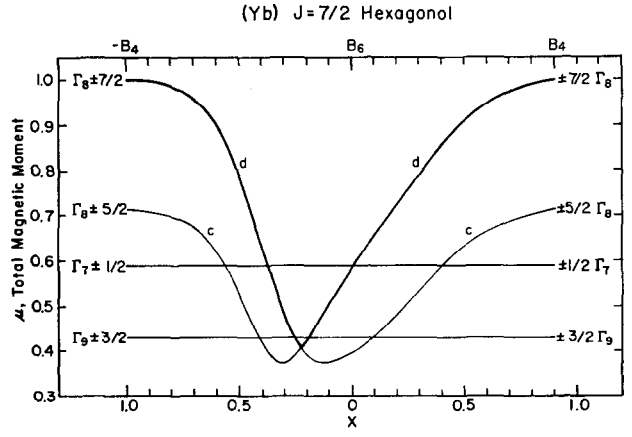

FIG. 14. Data corresponding to that in Fig. 4 for ion with $J = 7/2$.

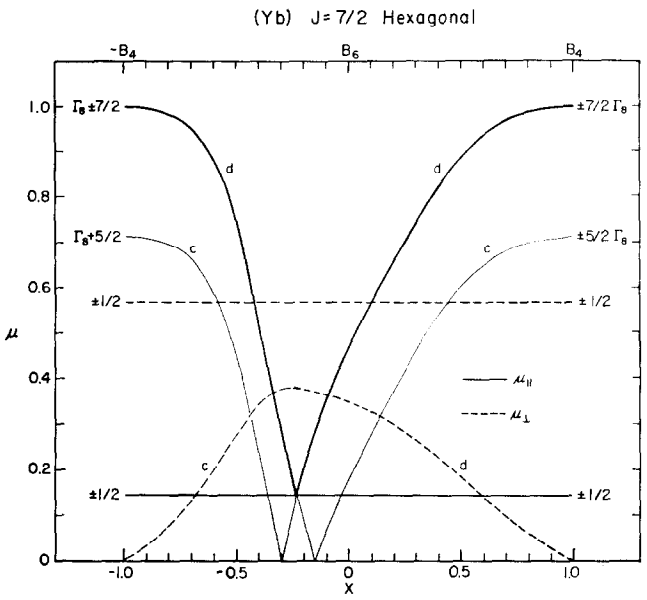

FIG. 15. Data corresponding to that in Fig. 5 for ion with $J = 7/2$.

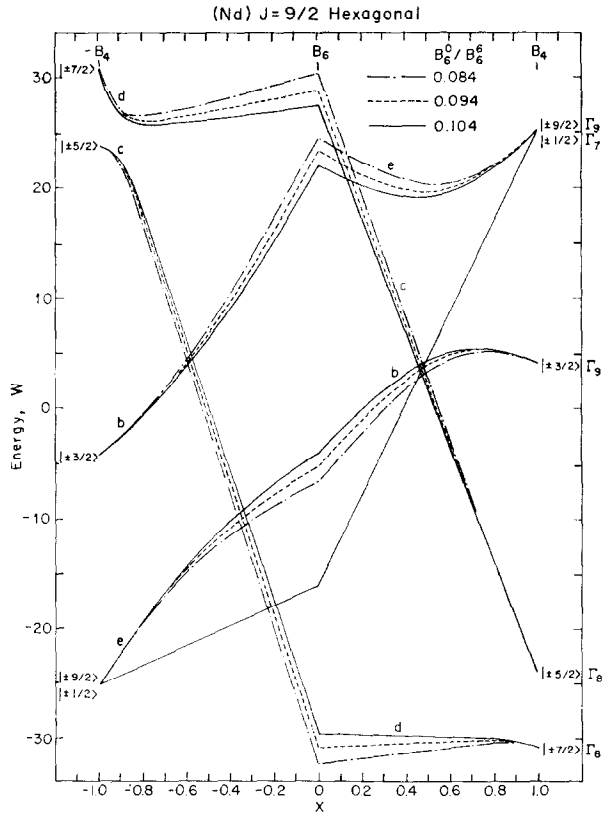

FIG. 16. Data corresponding to that in Fig. 8, for different B_6^0/B_6^6 values.

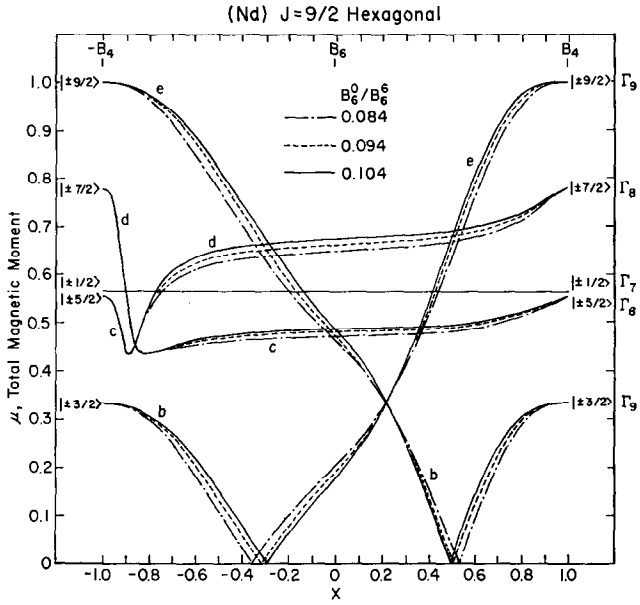

FIG. 17. Data corresponding to that in Fig. 9, for different B_6^0/B_6^0 values.

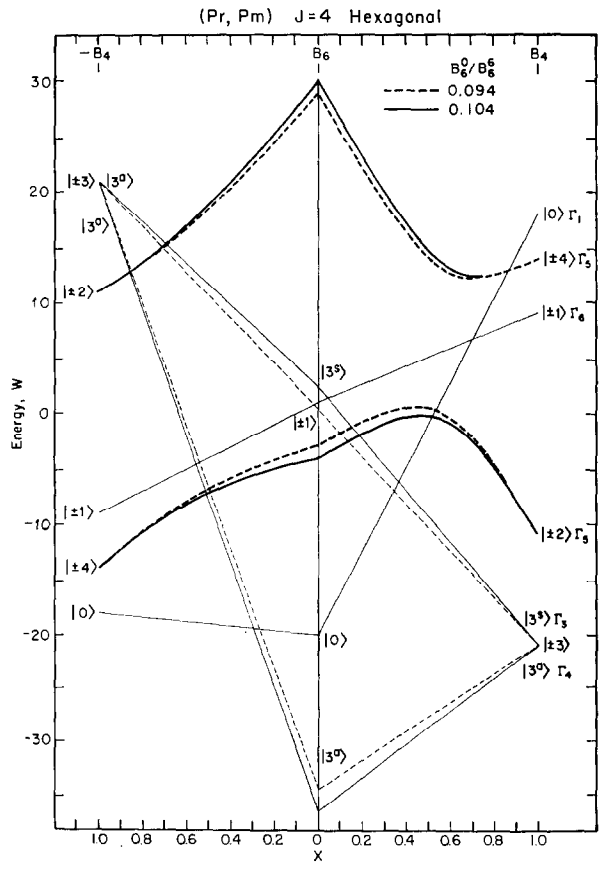

FIG. 18. Data corresponding to that in Fig. 11 for different B_6^0/B_6^0 values.

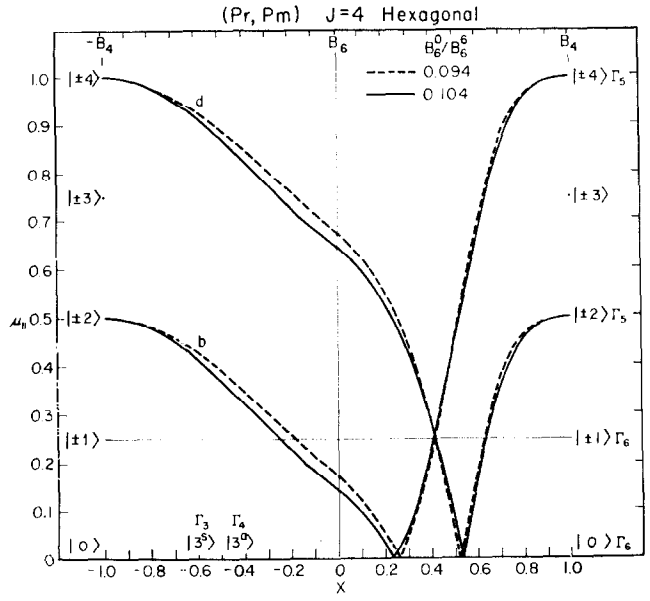

FIG. 19. Data corresponding to that in Fig. 12 for different B_6^0/B_6^0 values.

Laboratory dealing with the susceptibilities and heat capacity behavior of intermetallic compounds containing rare-earth elements (*4–6*, *9*, *21*, *22*).

References

1. D. H. PARKINSON, F. E. SIMON, AND F. H. SPEDDING, *Proc. Roy. Soc. Ser. A* **207**, 137 (1951).
2. W. G. PENNEY AND R. SCHLAPP, *Phys. Rev.* **41**, 194 (1932).
3. R. M. BOZORTH, B. T. MATTHIAS, H. SUHL, E. CORENZWIT, AND D. D. DAVIS, *Phys. Rev.* **115**, 1595 (1959).
4. W. E. WALLACE, "Progress in Rare Earth Science and Technology," (L. Eyring, Ed.), Vol. 3, p. 1, Pergamon Press, New York, 1958.
5. W. E. WALLACE, F. KISSELL, E. SEGAL, AND R. S. CRAIG, *J. Phys. Chem. Solids* **30**, 13 (1969).
6. K. H. MADER, E. SEGAL, AND W. E. WALLACE, *J. Phys. Chem. Solids* **30**, 1 (1969).
7. J. A. WHITE et al., *Phys. Rev.* **131**, 1039 (1963).
8. K. R. LEA, M. J. M. LEASK, AND W. P. WOLF, *J. Phys. Chem. Solids* **23**, 1381 (1962).
9. T. TSUCHIDA AND W. E. WALLACE, *J. Chem. Phys.* **43**, 2087, 2885 (1965).
10. B. BLEANEY, *Proc. Roy. Soc. Ser. A* **276**, 39 (1963).
11. D. P. SCHUMACHER AND C. A. HOLLINGSWORTH, *J. Phys. Chem. Solids* **27**, 749 (1966).
12. Y. EBINA AND N. TSUYA, *Sci. Rep. Res. Inst. Tohoku Univ. Ser. Suppl. B* **15**, 1, 47 (1963).
13. R. J. ELLIOTT AND K. W. H. STEVENS, *Proc. Roy. Soc. Ser. A* **219**, 387 (1953).
14. C. A. HUTCHISON, JR. AND E. WONG, *J. Chem. Phys.* **29**, 754 (1958).
15. G. H. DIEKE, "Spectra and Energy Levels of Rare Earth Ions in Crystals," Interscience Publishers, New York, 1968.
16. M. T. HUTCHINGS, *Solid State Phys.* **16**, 277 (1966).
17. M. T. HUTCHINGS AND D. K. RAY, *Proc. Phys. Soc. London* **81**, 663 (1963).
18. Ref. (*15*), p. 148.
19. K. W. H. STEVENS, *Proc. Roy. Soc. Ser. A* **65**, 209 (1952).
20. E. SEGAL, *in* "Thermal, Structural and Magnetic Studies of Metals and Intermetallic Compounds" (W. E. Wallace and R. S. Craig, Eds.), Annual Report to the U.S. Atomic Energy Commission, NYO-3454-27, May 15, 1969.
21. W. E. WALLACE et al., CNRS Colloquium on Rare Earths, No. 180, Vol. II, 427 (1970).
22. W. E. WALLACE, R. S. CRAIG, AND C. DEENADAS, to appear.
23. H. BETHE, *Ann. Phys.* **3**, 133 (1929); English transl., Plenum Publishing Corp., New York.